THE JOURNAL OF BIOLOGICAL CHEMISTRY VOL. 291, NO. 42, pp. 22030–22042, October 14, 2016

Death-associated Protein Kinase-1 Expression and Autophagy in Chronic Lymphocytic Leukemia Are Dependent on Activating Transcription Factor-6 and CCAAT/Enhancer-binding Protein-β*

Received for publication, March 4, 2016, and in revised form, August 27, 2016 Published, JBC Papers in Press, September 2, 2016, DOI 10.1074/jbc.M116.725796

Padmaja Gade[‡], Amy S. Kimball[§], Angela C. DiNardo[‡], Priyamvada Gangwal[‡], Douglas D. Ross[§¶‖], H. Scott Boswell[**], Susan K. Keay[§‖], and Dhananjaya V. Kalvakolanu[‡1]

From the Departments of [‡]Microbiology and Immunology and [§]Medicine and the [¶]Greenebaum Comprehensive Cancer Center, University of Maryland School of Medicine, Baltimore, Maryland 21201, the [‖]Baltimore Veterans Affairs Medical Center, Baltimore, Maryland 21201, and the [**]Indianapolis Veterans Affairs Medical Center, Indianapolis, Indiana 46202

Expression of DAPK1, a critical regulator of autophagy and apoptosis, is lost in a wide variety of tumors, although the mechanisms are unclear. A transcription factor complex consisting of ATF6 (an endoplasmic reticulum-resident factor) and C/EBP-β is required for the IFN-γ-induced expression of *DAPK1*. IFN-γ-induced proteolytic processing of ATF6 and phosphorylation of C/EBP-β are obligatory for the formation of this transcriptional complex. We report that defects in this pathway fail to control growth of chronic lymphocytic leukemia (CLL). Consistent with these observations, IFN-γ and chemotherapeutics failed to activate autophagy in CLL patient samples lacking ATF6 and/or C/EBP-β. Together, these results identify a molecular basis for the loss of *DAPK1* expression in CLL.

Multiple genes are inactivated during the progression of a normal cell into malignant one. The death-associated protein kinase-1 (DAPK1) is a Ca^{2+}/calmodulin-dependent serine/threonine kinase that controls several aspects of cell growth, including cell cycle check points, apoptosis, and autophagy, and suppresses tumor metastasis (1–3). Expression of DAPK1 is frequently lost in a variety of solid and hematologic malignancies, including chronic lymphocytic leukemia (CLL)[2] (4). However, the precise molecular mechanisms of such loss are not known. CLL, a mature B cell malignancy, is one of the more prevalent types of adult leukemias. Limited therapeutic interventions are available for advanced stages, and, as a result, increased mortality of elderly patients occurs (5). A major proportion of CLL patients display abnormalities in cytokine secretion and/or response (6). For example, phytohemagglutinin-activated $CD2^+$ cells from CLL patients produced higher levels of IFN-γ and TNF-α compared with healthy individuals. Serum IL2 and IL4 levels were significantly higher in CLL patients than in the healthy controls (7).

IFNs promote cell cycle arrest, apoptosis, and autophagy by inducing a number of cellular genes (8, 9). The well described IFN-induced JAK-STAT pathways are critical for executing acute responses, such as antiviral activities. However, a number of other pathways regulate IFN-induced chronic biological activities, such as cell growth and adaptive immunity. Earlier, we identified a non-STAT pathway in which transcriptional factor CCAAT/enhancer-binding protein-β (C/EBP-β) promotes IFN-induced responses (10, 11). C/EBP-β is critical for the IFN-induced expression of *DAPK1* (12–14). Importantly, C/EBP-β cooperates with the activating transcription factor 6 (ATF6), a key ER stress-associated transcription factor, for inducing *DAPK1* expression in response to IFN-γ (15). We have shown that the IFN-induced threonine phosphorylation of C/EBP-β in its second regulatory domain by ERK1/2, along with the phosphorylation and proteolytic activation of ATF6, is obligatory for *DAPK1* expression (15, 16). Because most of these studies were restricted to mouse embryonic fibroblasts (MEFs), the relevance of this new pathway to human cancers is not clear. Here we examined the importance of this pathway to cell growth control via autophagy using a CLL model.

Autophagy, an intracellular vesicle-initiated, lysosome-dependent self-digestion, is emerging as a major mechanism for tumor suppression, pathogen elimination, removal of apoptotic cells, and antigen presentation (17). Autophagy appears to play a dual role in cancer cells. It promotes cancer cell survival by supplying energy sources. In contrast, it serves as an effective tumor-suppressive mechanism due to excessive digestion of cellular contents (18).

Although one major mechanism for *DAPK1* silencing in cancer appears to be promoter methylation, it is often silenced without apparent methylation in many cases (19). Mutational inactivation of *DAPK1* is uncommon, except in the case of a familial form of CLL that diminishes its expression (20). In one case, this rare "CLL haplotype" resulted in an increased binding of the homeobox transcription factor HOXB7 to the *DAPK1* promoter, resulting in a slight but significant reduction of its expression (20). This aberration is not global to all CLLs. Thus,

* This work was supported by National Institutes of Health Grant CA78282 (to D. V. K.), and Cigarette Restitution funds from the University of Maryland Greenebaum Cancer Center. The authors declare that they have no conflicts of interest with the contents of this article. The content is solely the responsibility of the authors and does not necessarily represent the official views of the National Institutes of Health.

[1] To whom correspondence should be addressed. Tel.: 410-328-1396; E-mail: dkalvako@umaryland.edu.

[2] The abbreviations used are: CLL, chronic lymphocytic leukemia; MEF, mouse embryonic fibroblast; HDAC, histone deacetylase; qPCR, real-time quantitative PCR; NR-IgG, non-reactive rabbit IgG; PBL, peripheral blood lymphocyte; CDK, cyclin-dependent kinase.

there is a critical need to understand how DAPK1 expression is suppressed. We hypothesized that a dysfunction in the C/EBP-β and ATF6 pathway contributes to a loss of DAPK1 expression and growth control in CLL. We report here that defects in this pathway suppress DAPK1 expression and promote CLL growth.

Results

IFN-γ-stimulated Autophagy Correlates with DAPK1 Expression Levels in B Cells—We first investigated whether DAPK1 expression was induced by IFN-γ in B cell tumor line MEC1 (derived from a case of CLL) and compared it with a control B cell line. Western blotting analyses showed higher basal DAPK1 levels in the B cell line, which was further stimulated following IFN-γ treatment (Fig. 1*A*). Neither basal nor IFN-induced expression of DAPK1 was detected in MEC1. Similarly, *DAPK1* mRNA was induced following IFN-γ treatment, only in the control B cell line and not in MEC1 (Fig. 1*B*). Notably, even the basal *DAPK1* mRNA expression was significantly lower in this tumor line, compared with the control. Because DAPK1 participates in autophagy and tumor suppression, such a defect could result in an inhibition of autophagy. Initially, we examined the levels of Beclin1 (*BECN1*), a crucial regulator of autophagy and tumor suppression (Fig. 1*B*). No significant differences were observed in the basal and IFN-induced *BECN1* mRNA levels in the control B cell line and MEC1. Next, we investigated whether IFN-γ differentially stimulated autophagy in these cells by measuring the formation of LC3 puncta. IFN-γ induced significant LC3 puncta only in the control B cell line and not in the MEC1 cell line (Fig. 1*C*).

Alternatively, LC3-II formation, p62 (SQSTM1) degradation, and Beclin1 (Thr^{119}) phosphorylation levels were measured in these cells using Western blotting analyses with specific antibodies (Fig. 1*D*) to confirm activation of autophagy. The increase in formation of LC3-II correlated well with puncta formation in the control B cell line. The p62 (SQSTM1) protein cargoes oxidized protein aggregates to autophagosomes (21), which are degraded along with the cargo during autophagy. Thus, higher cellular p62 levels indicate a defect in autophagy. Upon IFN-γ treatment, p62 was lowered only in the control B cell line and not in MEC1 (Fig. 1*D*). Because DAPK1 is known to phosphorylate Beclin1 during autophagy (22), we next examined its phosphorylation at Thr^{119}. Although both cell lines expressed comparable levels of total Beclin, increased Beclin1-$Thr(P)^{119}$ was found only in the control B cell line and not in MEC1 in response to IFN treatment (Fig. 1*D*). To ensure the critical role of DAPK1 in autophagy, we investigated whether a knockdown of *DAPK1* using RNA*i* in the control B cell line and an introduction of *DAPK1* into MEC1 would alter autophagy. Fig. 1*E* shows the Western blotting analysis of DAPK1 levels in these cell lines along with their corresponding controls. Immunofluorescence analyses showed that DAPK1 depletion in the control B cell line caused a significant loss of the IFN-γ-induced LC3 puncta when compared with the scrambled shRNA control (*Sc shRNA*) (Fig. 1*F*). In contrast, DAPK1 expression in MEC1 yielded maximum LC3 puncta, compared with vector control, following IFN-γ treatment.

DAPK1 Expression in B Cell Lines Requires ATF6 and C/EBP-β—Because our recent studies using MEFs identified a major role for ATF6 and C/EBP-β in promoting DAPK1 expression, we investigated the relevance of these transcription factors (Fig. 2*A*) to DAPK1 expression in B cells, using RNAi. The ATF6- or C/EBP-β- specific shRNAs, but not the scrambled shRNA control, suppressed the IFN-induced expression of DAPK1 in B cells (Fig. 2*B*). Because the levels of the targeted proteins were not significantly different between mock-transfected and scrambled shRNA control-transfected cells (Fig. 2*A*), in the following experiments, all comparisons were made between scrambled shRNA control and specific shRNA transfectants. Immunofluorescence analyses showed that only B cells with scrambled shRNA control yielded maximum numbers of LC3 puncta upon IFN-γ treatment, when compared with either ATF6 or C/EBP-β depletion, signifying their importance in IFN-induced autophagy (Fig. 2*C*). Notably, we were able to co-localize LC3 puncta and DAPK1 in the IFN-treated control cells but not in ATF6- or C/EBP-β-depleted cells. Because certain histone deacetylases (HDACs), HDAC2 and HDAC5, were known to repress *DAPK1* in certain forms of acute myeloid leukemia (23), we measured their levels by Western blotting analysis and found that such differences were not due to an increased expression of HDACs in these cells when either ATF6 or C/EBP-β was depleted (Fig. 2*B*). To address whether the ATF6·C/EBP-β complex is recruited to the *DAPK1* promoter upon IFN-γ treatment, we performed ChIP assays with specific antibodies. *DAPK1* promoter-specific PCR products were observed only in the control B cell line and not in MEC1 following IFN-γ treatment (Fig. 2*D*). The control reactions with either no IgG or non-reactive rabbit IgG (NR-IgG) yielded no products, showing the specificity of the ChIP assay. Real-time quantitative PCR (qPCR) analysis of these ChIP products is shown in Fig. 2*E*. Thus, a failure to recruit ATF6 and/or C/EBP-β to the *DAPK*1 promoter may result in a loss of DAPK1 expression in the tumor cells.

We next examined the mechanistic bases for the lack of ATF6 and C/EBP-β recruitment to the *DAPK1* promoter in MEC1 cells. Because IFN-induced phosphorylation of C/EBP-β and proteolytic activation of ATF6 are required for DAPK1 expression, we checked whether any aberrations in these processes were responsible for the lack of transcription factor recruitment to the *DAPK1* promoter. Only the control B cells showed higher levels of phospho-Thr^{235} C/EBP-β (a known ERK-phosphorylated site) and activated ATF6 (50-kDa form) upon IFN-γ treatment (Fig. 2*F*). Strikingly, phospho-Thr^{235} C/EBP-β was barely detectable in MEC1 cells, whereas normal proteolytic activation of ATF6 was detected in MEC1 tumor cells upon IFN-γ treatment. Bar graphs in the *bottom panel* of Fig. 2*F* show the quantified data.

The importance of previously reported ERK and p38 MAPK signaling pathways for IFN-γ-induced C/EBP-β·ATF-6-dependent DAPK1 expression was examined in B cell lines by using chemical inhibitors. We used PD98059 and SB20219 for specifically blocking the activation of ERK1/2 and p38 MAPK, respectively. An unrelated inhibitor that blocks the PI3K pathway was used as a control. The effects of these inhibitors on the *DAPK1* mRNA levels in B cells and MEC1 tumor cells were

studied. Only PD98059 and SB20219 and not the control inhibitor LY294002 or DMSO blocked the IFN-induced *DAPK1* mRNA levels in B cells (Fig. 2*G*). However, in MEC1 cells, as predicted, IFN-γ treatment did not yield any significant differences in the presence or absence of specific inhibitors. In the next experiment, we investigated whether the ATF6·C/EBP-β

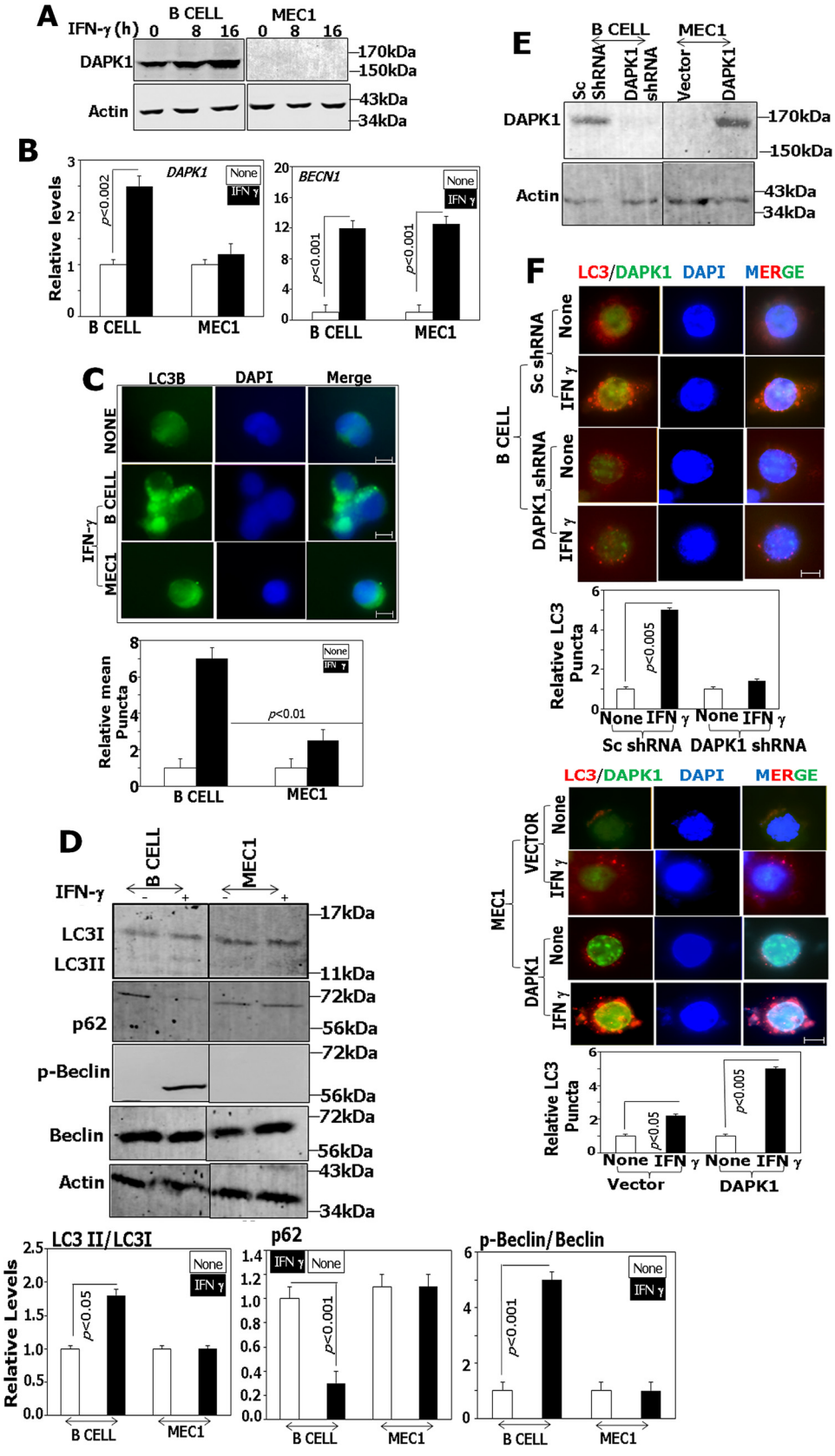

complex is recruited to the *DAPK1* promoter upon IFN-γ treatment in the presence of these inhibitors. We performed ChIP assays with specific antibodies. qPCR analyses of the ChIP products are shown in Fig. 2*H*. Only the specific inhibitors PD98059 and SB20219 and not the DMSO control blocked the IFN-induced recruitment of ATF6 and C/EBP-β to the *DAPK1* promoter.

Loss of DAPK1 Expression Correlates with That of ATF6/CEBPB in CLL—To examine the clinical relevance of the above observations, we investigated whether a correlation exists between DAPK1 levels and ATF6 or C/EBP-β expression in primary CLL. The patient sample details are shown in Table 1. Because we could only obtain small quantities of purified primary tumor cells, we measured expression levels of the stated mRNA by qPCR. Peripheral blood lymphocytes (PBLs) from healthy individuals ($n = 8$) were used as a control in these experiments. qPCR analyses of the steady state levels of *DAPK1*, *ATF6*, *BECN1*, and *CEBPB* mRNAs in the patient samples showed a loss of their expression in the majority of CLLs (Fig. 3*A*). Unlike in the MEC1 tumor cell line, many CLL samples also expressed a significantly lower level of *BECN1* when compared with the controls.

Because ATF6 is also involved in ER stress responses, we investigated changes in the mRNA levels of ER stress response genes, such as *HSPA5* (*BiP*), *ATF4*, and *XBP1*. Both *HSPA5* and *ATF4* levels were significantly low in many samples. No significant changes in *XBP1* levels were observed in these samples (Fig. 3*B*). We also investigated whether there were any differences in mRNA levels of IFN-induced tumor suppressor genes *IRF1* and *IRF8* (24, 25). These transcripts were abundantly expressed in CLL samples, and their levels were comparable with those of healthy controls (Fig. 3*B*).

Fig. 3*C* shows the relative abundance of *DAPK1*, *ATF6*, and *CEBPB* mRNAs in each CLL sample. Although two samples (patients A and J) expressed normal levels of *CEBPB*, they had a lower level of *ATF6*. In another sample (patient C), *ATF6* and *CEBPB* mRNA levels were similar and lower, respectively, compared with controls. Thus, low *DAPK1* levels correlated with severely reduced expression of either *ATF6* or *CEBPB* (except for one from patient B).

To address whether the ATF6·C/EBP-β complex is recruited to the *DAPK1* promoter upon IFN-γ treatment in the patient samples, we performed ChIP assays with specific antibodies. *DAPK1* promoter-specific PCR products were observed only in the control PBL and not in the patient samples ($n = 5$) following IFN-γ treatment (Fig. 3*D*).

ATF6 and C/EBP-β Are Essential for Driving IFN-induced DAPK1-dependent Autophagy in CLL—Because ATF6 and C/EBP-β are required for IFN-γ stimulated DAPK1 expression and autophagy, we next checked the expression levels of these proteins by immunofluorescence in different CLL patient samples. Fig. 4*A* shows the representative images for the levels of DAPK1, C/EBP-β, and ATF6 from CLL samples (different patient samples) alongside a healthy control. After immunostaining with specific antibodies, images were captured, and mean fluorescence intensity of the signals was determined using ImageJ (National Institutes of Health). As observed in qPCR profiles, DAPK1, ATF6, and C/EBP-β levels were very low in CLL patient samples when compared with healthy controls. In some samples (B, F, and J), for which sufficient cell numbers were available, we quantified DAPK1 levels using Western blotting analyses (Fig. 4*B*). CLL samples F and J did not express DAPK1. In patient sample B, where a high level of steady state DAPK1 was observed, IFN-γ treatment did not induce DAPK1 levels further. As expected, normal PBL control(s) expressed both steady state and IFN-γ-induced DAPK1 (Fig. 4*B*).

In the subsequent experiments, we investigated the effects of flavopiridol, a pan-cyclin-dependent kinase (CDK) inhibitor (26), and chlorambucil, an alkylating agent (27), which demonstrated significant clinical activity in CLL (28, 29), on autophagy and cell growth. Fig. 4*C* (*top panels*) shows Western blotting analyses of LC3-II p62, phospho-Beclin1, and Beclin1 levels in the indicated CLL samples after IFN-γ (for 8 h), flavopiridol (2 μM for 4 h), and chlorambucil (20 μM for 4 h) treatments. LC3-II formation was severely suppressed in the three CLL samples compared with healthy control PBL. p62 levels were either greater than or the same relative to the untreated control, consistent with the ablation of autophagy in the CLL samples. Consistent with these observations, phospho-Beclin1 levels were also undetectable in all CLL samples when compared with the control PBL. Fig. 4*C* (*bottom*) shows the quantified data for each of the proteins analyzed. Thus, a loss of expression of ATF6 and/or C/EBP-β results in severely reduced autophagy in CLL.

Because DAPK1 is a regulator of cell death, we also measured the percentage of viable cells in the tumor and control B cell lines following treatment with IFN-γ, flavopiridol, and chlorambucil (Fig. 4*D*). Upon IFN-γ treatment (for 4 or 16 h), the percentage of viable cells significantly declined in the control B cell line but not in MEC1. Similarly, flavopiridol and chlorambucil treatment significantly suppressed the viability of the control B cell line but not MEC1. In summary, the tumor cell line MEC1 defective for C/EBP-β phosphorylation (see Fig. 2) showed a poorer response to IFN-γ and therapeutic agents. A similar experiment could not be performed in primary CLL samples due to the limited availability of cells.

FIGURE 1. **Loss of IFN-γ-stimulated autophagy and DAPK1 expression in MEC1, a B cell CLL cell line, compared with a control non-oncogenic B cell line.** *A*, Western blotting analyses of cell lysates with the indicated antibodies. Cell types and time points of treatment (IFN-γ, 500 units/ml) are indicated. *B*, qPCR analyses of *DAPK1* and *BECN1* transcripts. Cells were treated with IFN-γ for 12 h. $n = 5$/sample. *C*, *top panels*, immunofluorescence signals of LC3 (FITC; *green channel*). The nucleus is stained with DAPI (*blue channel*). *Scale bar*, 10 μm. *Bottom panel*, quantified relative mean puncta after background correction. *Bars*, mean ± S.D. (*error bars*) ($n = 3$, 10 independent fields/sample). Relative levels were calculated with respect to those obtained with the untreated control. *D*, *top panels*, Western blotting analyses of lysates with the specific antibodies. Specific cells and treatments (IFN-γ for 12 h) are indicated. *Bottom*, histograms show relative intensities of the bands after normalization to its actin internal control. *E*, Western blotting analyses of lysates from the indicated cell lines. Specific genes transfected are also indicated. *F*, immunofluorescence signals of DAPK1 (FITC, *green channel*) and LC3 (Alexa Fluor 568, *red channel*). The nucleus is stained with DAPI (*blue channel*). *Scale bar*, 10 μm. Treatment was with IFN-γ for 12 h. Typical images and quantified mean puncta after background correction are shown. *Bars*, mean ± S.D. ($n = 3$; 10 independent fields/sample).

Restoration of C/EBP-β and ATF6 into CLL Patient Samples Reestablishes IFN-γ-induced DAPK1 Expression and Autophagy—We next examined whether restoration of C/EBP-β and/or ATF6 in the defective CLL patient samples would reestablish DAPK1 expression and autophagy. For this experiment, we have chosen two CLL patient samples: 1) sample F with a low C/EBP-β but a normal ATF6 level and 2) sample J with low ATF6 but a normal C/EBP-β level. These cells were transfected

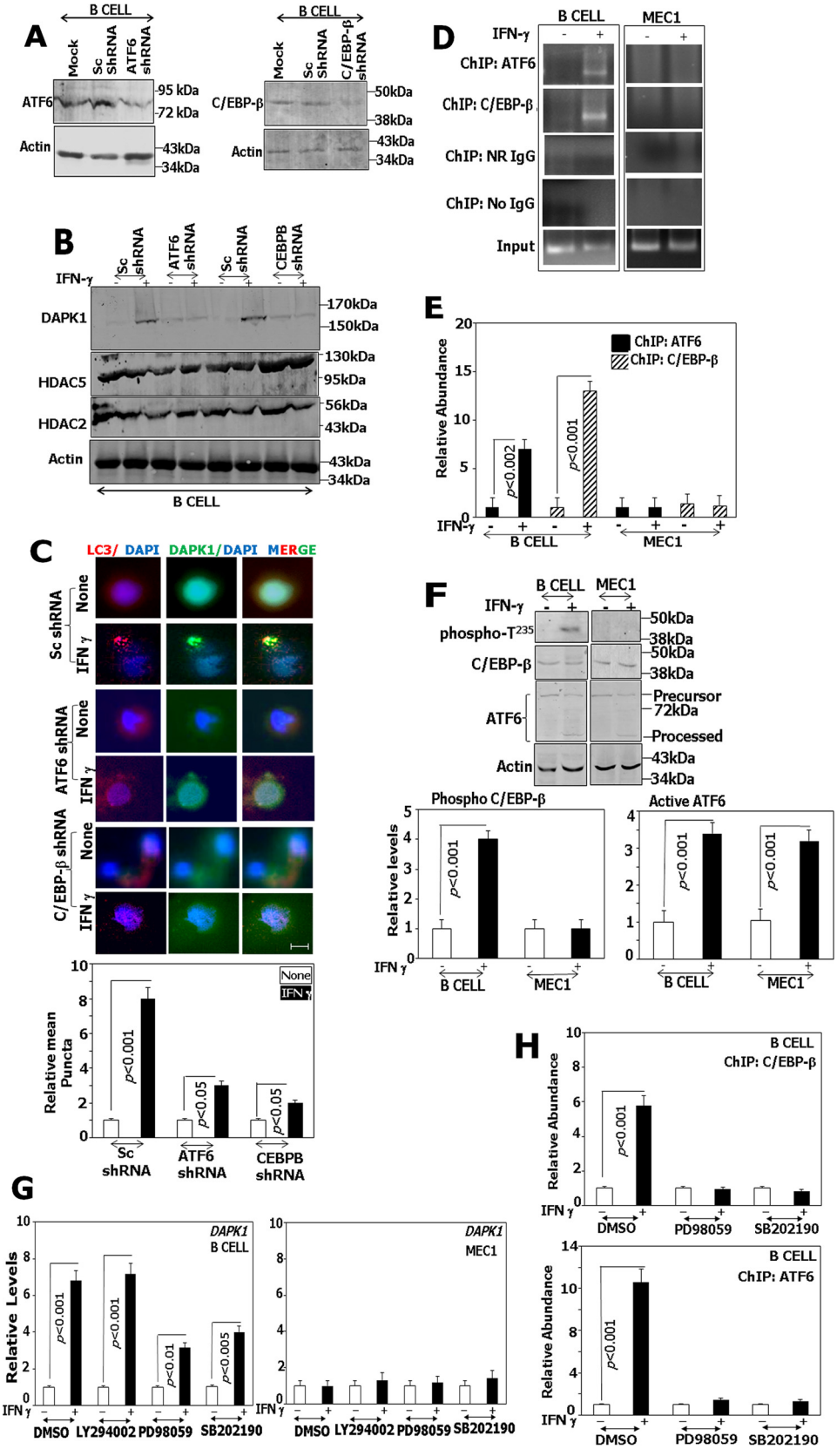

TABLE 1
Details of CLL samples obtained from patients

Patient sample	Gender	Age	Ethnicity
		yr	
A	Male	84	Caucasian
B	Male	58	Caucasian
C	Male	68	Caucasian
D	Male	62	Caucasian
E	Male	45	African-American
F	Female	66	African-American
G	Male	72	Caucasian
H	Male	39	Caucasian
I	Female	60	Caucasian
J	Male	41	African-American
K	Female	64	African-American
L	Male	65	Caucasian
M	Female	64	African-American
N	Male	56	Asian/Pacific Islander
O	Male	62	Caucasian
P	Male	62	Caucasian
Q	Male	61	Caucasian
R	Male	59	African-American
S	Male	72	Caucasian
T	Male	59	Caucasian
U	Male	71	Caucasian

with lentiviral expression vectors encoding either C/EBP-β (F) or ATF6 (J) or control vector alone (F and J) (Fig. 5*A*). These cells were examined for IFN-induced expression of DAPK1 and autophagy. IFN-γ was able to induce DAPK1 expression and promote autophagy (Fig. 5, *B* and *C*) only after a re-expression of C/EBP-β or ATF6 in these CLL samples.

Discussion

Autophagy maintains cellular hygiene by eliminating damaged organelle or protein aggregates via sequestration into double membrane intracellular vesicles and their subsequent fusion with lysosomes. Autophagy has been linked to both survival and death (30), depending on the cell type, signal, and physiologic state of a cell (31). For example, autophagy promotes cell survival by providing nutrients during cell starvation. In contrast, it can promote cell death via excessive digestion organelles if cells fail to return to normal functions. Autophagy promotes senescence to suppress tumor growth (32–34). Blockade of autophagy enhances the apoptotic cell death mode in some cases. Indeed, a number of regulators of autophagy also participate in apoptosis (35). DAPK1 is one of the first known proteins that directly connects autophagy to cell death through phosphorylation of Beclin1, a known tumor suppressor (36). DAPK1 employs several substrates for exerting its biological effects (37). For example, it phosphorylates and activates protein kinase D, a tumor suppressor that regulates *trans*-Golgi trafficking. During oxidative stress, DAPK1 binds and phosphorylates Vps34, a major regulator of autophagy (38). Importantly, DAPK1 phosphorylates Beclin1 at Thr^{119} to promote its dissociation from Bcl-X_L and induction of cell death via autophagy (36). Consistent with its tumor-suppressive effects, *DAPK1* expression is lost in a variety of cancers, including CLL (4). Overexpression of DAPK1 in the absence of p53 resulted in autophagic cell death in some hepatoma cell lines (2). In estrogen receptor-negative breast tumors with wild-type p53, DAPK1 serves as a death inducer. In contrast, in the p53 mutant background, DAPK1 functions as a growth promoter (39), although the precise mechanisms are unclear at this time. Although many studies reported a loss of DAPK1 expression in human tumors, the molecular bases have not been understood. In a previous study (23), we reported that *DAPK1* transcription is repressed by p52 NF-κB and histone deacetylases in the Flt3-ITD^+ subset of acute myeloid leukemias. This mechanism does not appear to hold true in the case of CLL, a genetically and cytologically distinct disease.

CLL is a progressive B cell malignancy that exhibits heterogeneity in its biology, progression, and overall survival of patients (41). Currently, very few effective therapeutics are available for treating CLL. Thus, an understanding of the molecular processes involved in this disease will pave the way for the development of new drugs. One major reason for cell survival seems to be defects in IFN-induced autophagy in CLL. Consistent with this, Beclin1-Thr^{119} phosphorylation and the degradation of p62 (SQSTM1) protein were defective in MEC1 cells (Fig. 1). The p62 (SQSTM1) protein, which cargoes oxidized protein aggregates and tethers them to LC3-like proteins, is also degraded during autophagy (21). In DAPK1-deficient cells, p62 accumulated, indicating an abrogation of autophagy. The resultant rise in p62 levels further increases oxidative stress and DNA instability (42, 43). DAPK1 interacts with MAP1B, which in turn binds with high affinity to LC3 (1). Both DAPK1 and MAP1B co-localized with α-tubulin and actin microfilament (1). Such mechanisms may allow the sliding of the autophagosomes along the cytoskeletal structures, culminating in their fusion with lysosomes.

The ER not only serves as an organelle for the synthesis and export of secreted and cell surface proteins but is also critical for executing autophagy. Extreme perturbations in ER homeostasis cause cell death (44). $Dapk1^{-/-}$ MEFs showed protection against tunicamycin (an ER stress inducer)-induced cell death (3). These cells not only respond poorly to ER stress but also exhibit defects in autophagy. How ER stress is coupled to autophagy is not clear. ATF6 is an ER-resident transcription factor, whose N-terminal half serves as a transcription factor, whereas its C-terminal half is a sensor of ER stress (45). In

FIGURE 2. **DAPK1 expression is critically dependent on ATF6 and C/EBP-β.** *A* and *B*, Western blotting analyses of the lysates with the indicated antibodies are shown. Specific genetic alterations of cells and/or treatments (IFN-γ for 12 h) are also indicated. *C*, *top*, immunofluorescence images of DAPI (nuclear stain), DAPK1 (FITC; *green channel*), and LC3 (Alexa Fluor 568; *red channel*). *Scale bar*, 10 μm. Treatment was with IFN-γ for 12 h. *Bottom*, quantified relative mean puncta after background correction. *Bars*, mean $\pm$ S.D. (*error bars*) ($n = 3$, 10 independent fields/sample). Relative levels were calculated with respect to those of untreated control values. *D*, ChIP assays. IFN-γ treatment was for 12 h. In each case, the soluble chromatin was used as input control. The typical ChIP-PCR patterns with DAPK1 enhancer-specific primers are shown. *E*, qPCR analyses of the ChIP products. Specific immunoprecipitation products were quantified, and the values were plotted as relative abundance with respect to the NR-IgG control ($n = 6$). *F*, *top panels*, Western blotting analyses of lysates with the indicated antibodies. Cells were treated with IFN-γ for 12 h. *Bottom*, histograms show relative intensities of the bands after normalization to those of internal control, actin. *G*, qPCR analyses of *DAPK1* transcript. Cells were treated with IFN-γ in the presence of inhibitors (SB202190 (20 μM), PD98059 (25 μM), LY294002 (50 μM), or DMSO). Inhibitors were added to the cells 30 min before IFN treatment for 12 h ($n = 5$). *H*, qPCR analyses of the ChIP products. ChIP assays were performed in the B cell line in the presence of the indicated inhibitors. IFN-γ treatment was for 12 h. In each case, the soluble chromatin was used as input control. PCR products were quantified, and the values were plotted as relative abundance with respect to the NR-IgG control ($n = 6$).

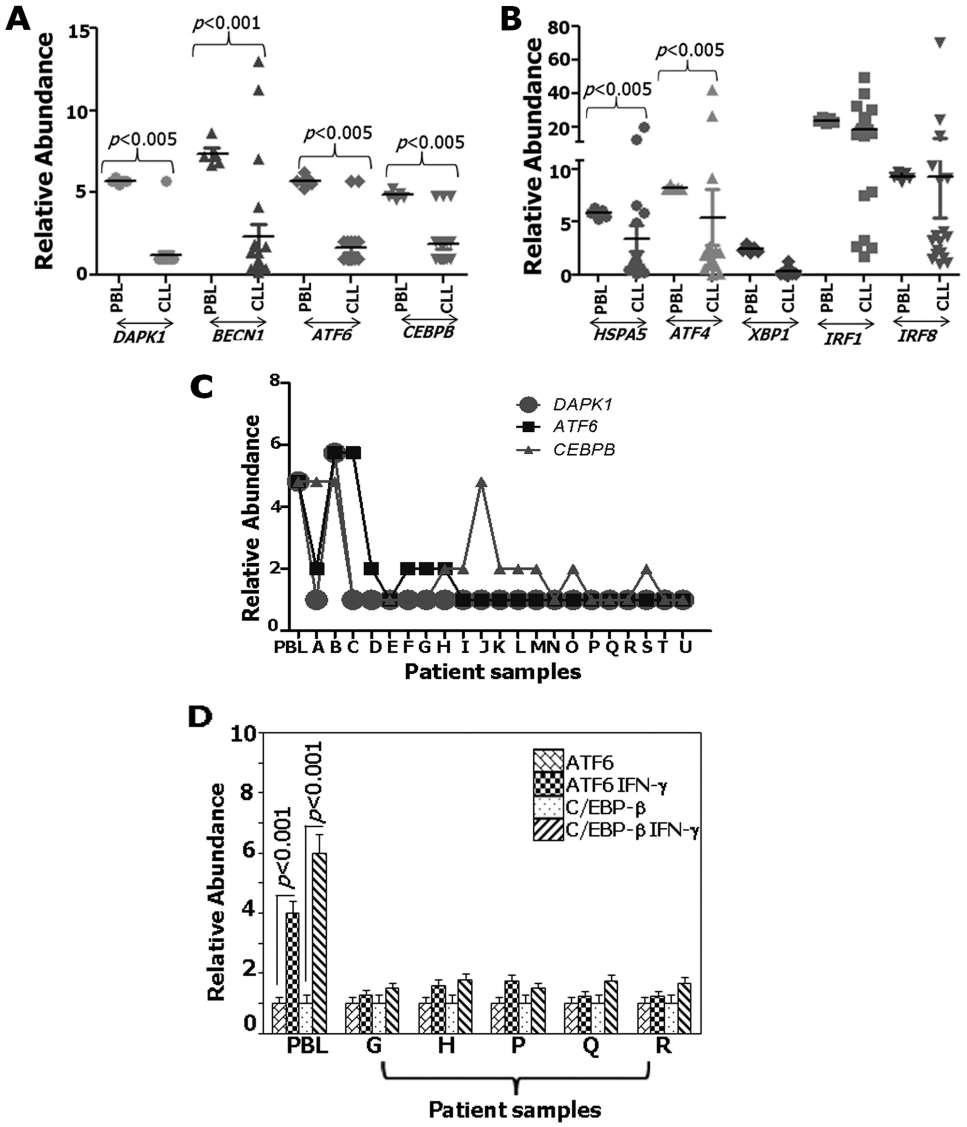

FIGURE 3. **Loss of *DAPK1* expression correlates with those of *ATF6* and *CEBPB* in primary CLL.** *A* and *B*, RNA was isolated from CLL patient samples as described under "Experimental Procedures," and qPCR analyses with the transcript-specific primers (listed in Table 2) were performed. The dot plots show relative abundance of the indicated transcripts (normalized to the internal control, ribosomal protein L32). Transcript abundance was calculated on the basis of threshold cycle values. Each *dot* shows the mean of each sample. $n = 5$ for PBL; $n = 21$ for CLL. *C*, plot showing relative abundance of the indicated transcripts in each CLL sample. *D*, qPCR analyses of the ChIP products. ChIP assays were performed in CLL samples in the presence and absence of IFN-γ. IFN-γ treatment was for 12 h. In each case, specific immunoprecipitation products were quantified, and the values were plotted as relative abundance with respect to the NR-IgG control ($n = 6$). *Error bars*, S.D.

response to ER stress, ATF6 translocates to the Golgi apparatus, where it is cleaved by resident proteases S1P and S2P. This process releases the active transcription factor part from the C-terminal portion. The former enters the nucleus and turns on the expression of specific genes (46). We have recently identified a unique pathway in which IFN-γ stimulated proteolytic activation of ATF6- and ERK1/2-induced phosphorylation on C/EBP-β converge to up-regulate *Dapk1* in MEFs (10, 15). In the present study, we show that this pathway is defective in CLL. C/EBP-β and ATF6 binding to the *DAPK1* promoter upon IFN treatment was found only in the control B cell line and not in the CLL cell line. Specifically, IFN-induced phosphorylation of C/EBP-β Thr^{235} was absent in the CLL cell line (Fig. 2). We demonstrated earlier that this site is a classic target for ERK1/2 enzymes. Consistent with this, inhibition of ERK1/2 decreased IFN-γ-induced C/EBP-β-dependent DAPK1 expression in the control B cell line. Similarly, we have recently reported that p38 MAPK-induced phosphorylation of ATF6 is required before its cleavage in the Golgi apparatus (15, 16). Indeed, blockade of p38 MAPK also inhibited IFN-induced DAPK1 expression.

The pathological relevance of this pathway was further supported by the observation that low levels of either *ATF6* or *CEBPB* correspond to low *DAPK1* expression in primary CLLs (Fig. 3). More importantly, restoration of the missing factors into primary tumors reinstated DAPK1 expression and autophagy (Fig. 5). It is likely that defects occur at multiple levels in the ATF6·C/EBP-β-dependent DAPK1 pathway in CLL. In the cell line model, C/EBP-β phosphorylation was found to be defective. In the primary CLLs analyzed

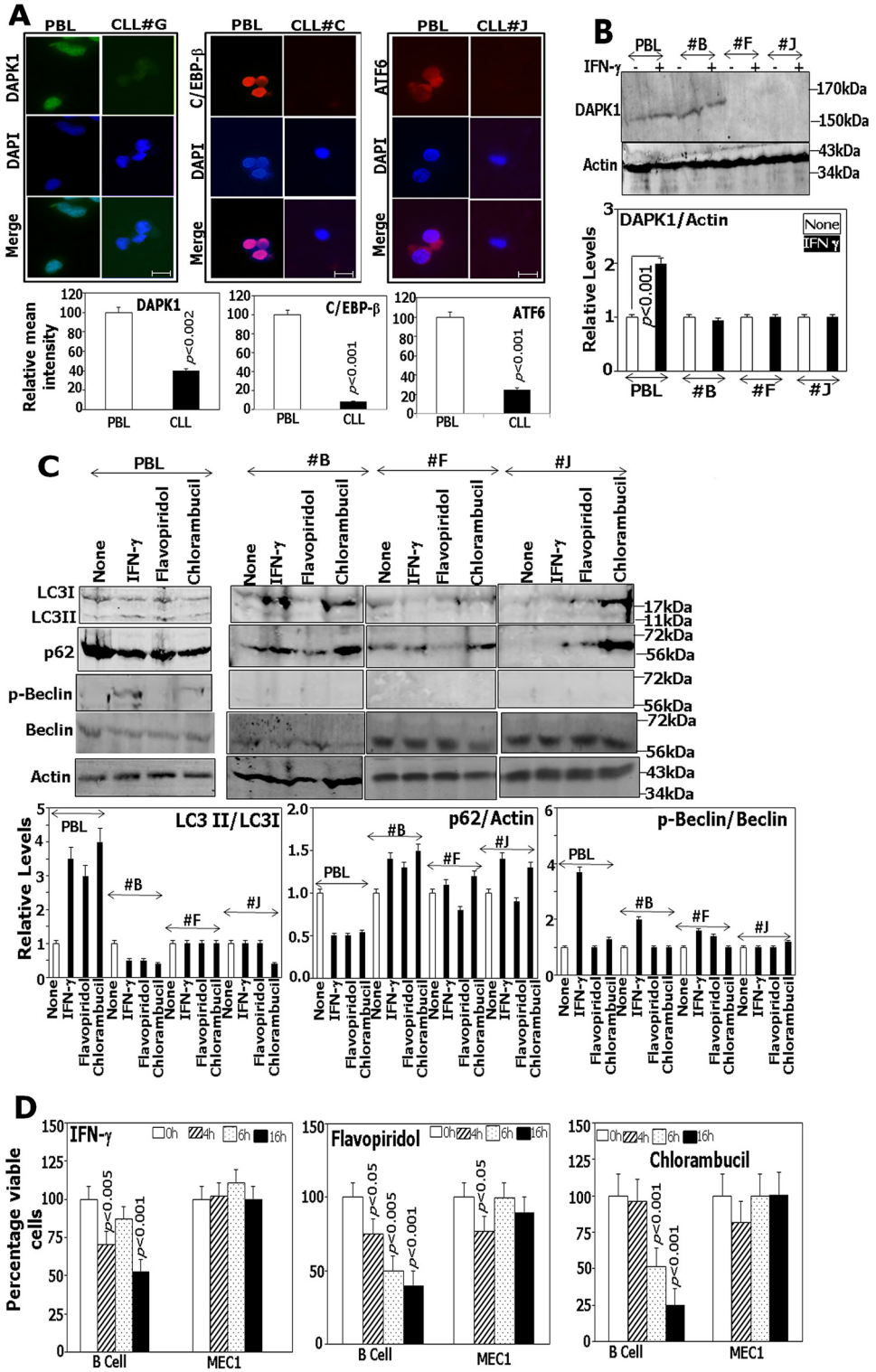

FIGURE 4. **Critical role for ATF6/C/EBP-β in driving IFN-induced autophagy in CLL.** *A*, *top panels*, immunofluorescence images of LC3 (FITC; *green channel*) and C/EBP-β·ATF6 (Alexa Fluor 568; *red channel*). DAPI was used to stain the nucleus (*blue channel*). *Scale bar*, 15 μm. Representative images from three different patient samples are shown. *Bottom*, histograms show quantified fluorescence (Alexa Fluor 568 (*red*) or FITC (*green*) from three different patient samples after background correction. *Bars*, mean $\pm$ S.D. of 10 independent fields per sample). *B* and *C*, *top panels*, Western blotting analyses of lysates with the indicated antibodies. Specific patient samples and treatments along with their controls are indicated: IFN-γ for 12 h, flavopiridol for 4 h, and chlorambucil for 4 h. *Bottom*, histograms show the relative intensities of the bands after normalization to actin control. *D*, viability of the cell lines after specific treatments (IFN-γ, flavopiridol, or chlorambucil) at the indicated time points. Experiments were performed in triplicate, and results are reported as mean $\pm$ S.D. (*error bars*).

here, we noted a decline in ATF6 and/or C/EBP-β levels. This does not mean that C/EBP-β phosphorylation is irrelevant to primary CLL. Like many cancers, CLL is a heterogeneous disease. Thus, it is important to examine these findings in a larger cohort of patient samples before arriving at such an inference.

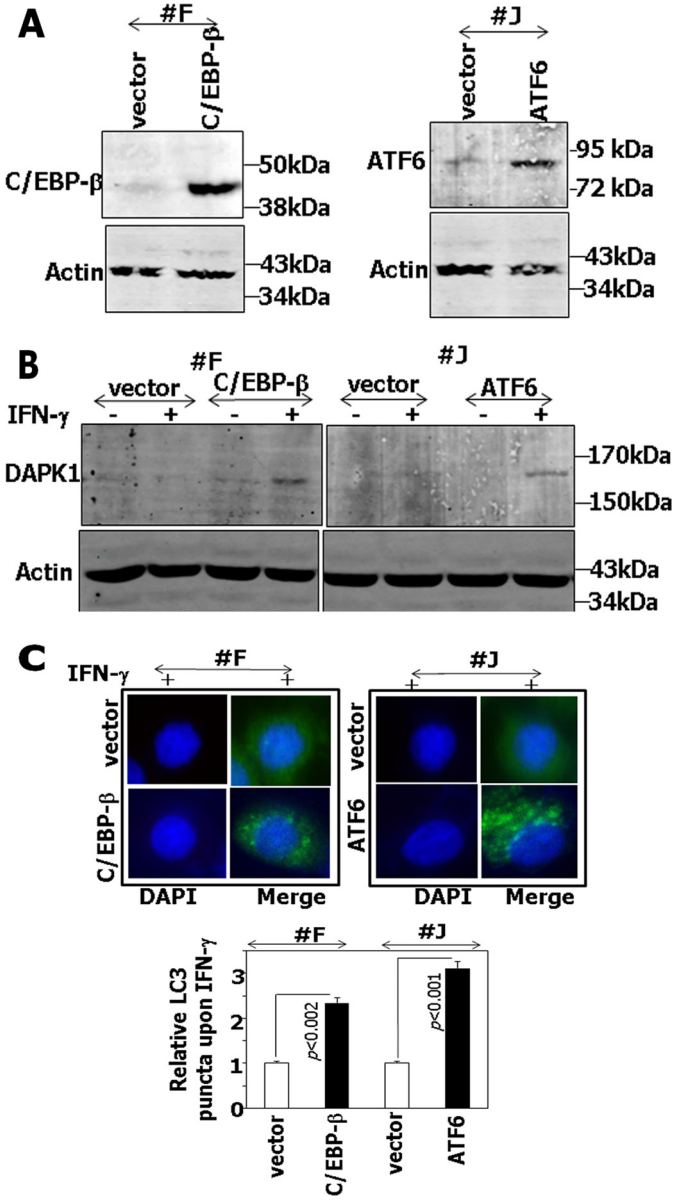

FIGURE 5. **Re-expression of C/EBP-β and ATF6 into CLL patient samples restores autophagy.** *A* and *B*, specific patient samples were transfected either with vector alone or C/EBP-β or ATF6 expression vectors and were analyzed by Western blotting with specific antibodies. IFN-γ treatment was for 12 h. *C*, *top panels*, fluorescence signals of nucleus (DAPI; *blue channel*) and LC3 (FITC; *green channel*). *Scale bar*, 10 μm; IFN-γ for 12 h. *Bottom*, quantified relative fluorescence of LC3 (FITC; *green channel*) after background correction. *Bars*, mean $\pm$ S.D. (*error bars*) (10 independent fields/sample).

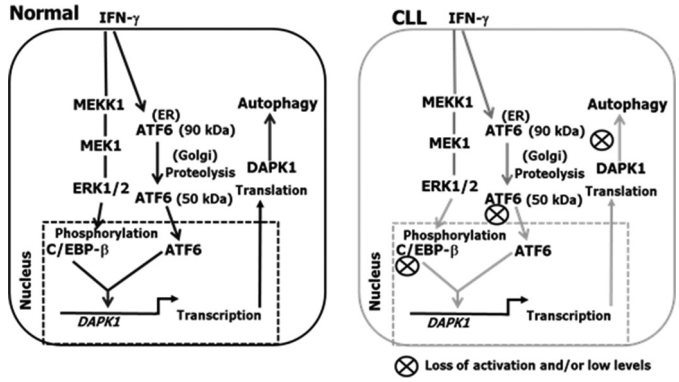

FIGURE 6. **A hypothetical model of IFN-induced DAPK1-driven CLL cell death.** In normal B cells, IFN-γ activates C/EBP-β through ERK1/2-dependent phosphorylation and ATF6 by proteolytic processing. A C/EBP-β·ATF6 complex recruits to the *DAPK1* enhancer and induces its expression and autophagy. In CLL, either low expression of these factors (C/EBP-β and/or ATF6) or loss of activation of C/EBP-β results in loss of collaboration of C/EBP-β and ATF6, which results in a failure to up-regulate optimal DAPK1 levels for the execution of autophagy.

ATF6, a major mediator of ER stress-driven transcription, binds to the ER stress response element in the target gene promoters, such as *BiP* (47). Additionally, upon ER stress, translational shutdown leads to selective translation of *ATF4* mRNA (48). Our data show that the ER stress response genes *HSPA5* and *ATF4* were significantly low in these CLL samples, indicating a poor ER stress response (Fig. 3). Defective autophagy caused a poorer anti-tumor response. Consistent with these reports, increase in LC3-II levels, p62 degradation, and DAPK1-dependent Beclin1 phosphorylation did not occur in primary CLL samples in response to IFN-γ, flavopiridol, or chlorambucil (Fig. 4). Importantly, re-expression of C/EBP-β and ATF6 in primary CLL samples resulted in restoration of IFN-induced DAPK1 expression and autophagy (Fig. 5). In light of these observations, we hypothesize that lower levels and/or aberrations in ATF6 and C/EBP-β activation may be prognostic for a poorer therapeutic response (Fig. 6) in CLL. That said, more detailed studies with a larger cohort of patients, whose therapeutic histories have been recorded, are required for arriving at a firmer conclusion. Such investigations are beyond the scope of the current study.

As mentioned above, autophagy acts both as a cell survival and a cell suicide mechanism, depending on the physiological condition and the type of cell. Cells with high basal autophagy tend to exhibit reduced sensitivity to chemotherapeutics, which has been inappropriately dubbed "drug resistance," a separate mechanism that actively pumps the drugs out using ABC transporters to minimize cytotoxicity (49). A recent study indicated that CDK-1/5 inhibition by flavopiridol induced autophagy and ER stress to block CLL growth (28). CDKs 1 and 5 have been shown earlier to negatively regulate autophagy (50) via a direct phosphorylation of Vps34 at its Thr^{159} residue, which blocked its interaction with Beclin1. Vps34 is an essential component of the Ambra1·UVRAG·Beclin1·Vps34·Vps15 complex that is necessary for the formation of autophagophore/omegasome, the precursor for autophagosome (51). Mahoney *et al.* (28) suggested that activation of the ER stress via the IRE1-TRAF2-ASK1-Caspase-4 axis by flavopiridol contributes to CLL death. We have shown here that DAPK1 induction via ATF6 is critical for suppressing cell survival. DAPK1 phosphorylation of Beclin1 is an important step in the execution of growth-suppressive autophagy (36). We have reported recently that DAPK1 expression is controlled by an ASK1-dependent phosphorylation of ATF6, which then allows its proteolytic cleavage in the Golgi and nuclear migration (15, 16). Thus, the IRE1-TRAF2-ASK1 and the ASK1-ATF6-DAPK1 axes may complement each other in promoting cell growth suppression in response to flavopiridol.

Some studies suggested an important role for microenvironment, where CLL expands within pseudofollicles. Stromal cells,

vascular endothelial cells, monocyte-derived nurse-like cells, and Th1 cells have been suggested to promote survival, proliferation, and migration of CLL cells (52–55). A recent study suggested that Th1-derived IFN-γ induced cell surface CD38 expression, via the JAK-STAT pathway, and requires the participation of transcription factor T-bet (56). CD38 is associated with CLL cell proliferation. The pathway used for up-regulating DAPK1 is distinct from the one used for inducing CD38. For example, DAPK1 expression does not require STAT1. Unlike CD38, DAPK1 promotes cell death and autophagy. One distinction between our study and that of Burgler *et al.* (57) is the absence of other cell types that create pseudofollicles because tumor cells used in the present study were derived from B cells enriched from peripheral blood. Despite these distinctions, our studies are not at odds with each other; gain and loss of CD38 and DAPK1, respectively, complement each other, in promoting CLL growth. Whether these two events occur simultaneously or at different stages of CLL evolution is an interesting question to be examined. The limited cell numbers obtained from CLL patients and lack of bone marrow samples from the same patients currently do not permit us such a rigorous examination of such issues at this time.

Meanwhile, our results suggest that regulation of autophagy via ATF6-C/EBP-β may be an important contributor to the suppression of CLL growth. Apart from C/EBP-β, ATF6 is also down-regulated during prostate cancer progression (58). A missense SNP in ATF6 is associated with the progression of hepatocellular carcinoma (59). C/EBP-β is also down-regulated in some human hepatocellular carcinomas (60). In sum, our studies for the first time couple ATF6·C/EBP-β to a major tumor suppressor, DAPK1, in CLL.

Experimental Procedures

Cell Lines and Other Reagents—An Epstein-Barr virus-immortalized human B cell line (CHS International Research Ltd., Orange, CA) (61) was grown in RPMI 1640 supplemented with 10% fetal bovine serum and 1% antibiotic-antimycotic agents. This cell line is non-oncogenic and does not exhibit any growth abnormalities. Because it expresses DAPK1 like normal PBLs, we used it as a control. MEC1, a CLL cell line (62), was cultured in McCoy's 5A medium. The ERK pathway inhibitor PD98059 and the PI3K inhibitor LY294002 were from EMD Millipore (Billerica, MA). p38 MAPK inhibitor SB202190, chlorambucil, and flavopiridol were from Sigma-Aldrich. Human IFN-γ was from PBL Inc. (Piscataway, NJ). Antibodies specific for DAPK1 were from Sigma-Aldrich. Rabbit antibodies against the phospho-Thr^{235} form of C/EBP-β were provided by Peter Johnson (NCI, National Institutes of Health, Frederick, MD). Rabbit antibodies against ATF6 and C/EBP-β were from Santa Cruz Biotechnology, Inc. (Dallas, TX).

Primary CLL Samples—Blood samples were collected from subjects diagnosed with CLL, after informed consent, at the University of Maryland Greenebaum Cancer Center (Baltimore, MD) under an institutional review board-approved protocol. These patients included Caucasians and African-Americans of both sexes. The Accuspin® system-HISTOPAQUE-1077 (Sigma-Aldrich) was used for separating leukocytes from whole blood, and B cells were isolated using a pan-B cell enrichment kit (Stemcell Technologies Inc., Vancouver, Canada). In brief, undesired cells were removed with the use of tetrameric antibody complexes recognizing CD2, CD3, CD14, CD16, CD36, CD42b, CD56, CD66b, CD123, glycophorin A, and dextran-coated magnetic particles. Finally, CD5$^+$ CD19, CD20, and CD23 positive cells (>98% pure) were separated from the remaining population using specific antibodies and used for further analysis as described below. PBLs from normal volunteer blood were used as the control for comparing the data from CLL patients.

TABLE 2
Gene-specific primers used in qPCR

Primers	Sequence (5′ → 3′)
hDAPK1-F	TCTAAGCCCACAGTCTCAGT
hDAPK1-R	GGATCTCATAGGGCTCTTCT
hIRF1-F	CACCAAGAACCAGAGAAAAG
hIRF1-R	CTGTGAAGACACGCTGTAGA
hXBP1qF	TGCTGAGTCCGCAGCAGGTG
hXBP1qR	GCTGGCAGGCTCTGGGGAAG
hATF4 qF	GGGACAGATTGGATGTTGGAGA
hATF4 qR	ACCCAACAGGGCATCCAAGT
hBIP qF	TGACATTGAAGACTTCAAAGCT
hBIP qF	CTGCTGTATCCTCTTCACCAGT
hATF6 RTF1	TGAACTTCGAGGATGGGTTC
hATF6 RTR1	TCACTCCCTGAGTTCCTGCT
hBECLIN RTF1	AGGTTGAGAAAGGCGAGACA
hBECLIN RTR1	ATTGTGAGGACACCCAAGC
hC/EBP-β qF	GACAAGCACAGCGACGAGTA
hC/EBP-β qR	AGCTGCTCCACCTTCTTCTG
hIRF8-F	TGTGCAAAGGCAGGCCCAACAA
hIRF8-R	TCTTCCCCAAAGCACAGCACCA

qPCR—Transcript levels of specific genes were determined using specific primers as in our earlier studies (10, 16). Additional primers are described in Table 2. The ribosomal protein L32 (*RPL32*) mRNA was used as an internal control. Relative transcript abundance was calculated using the $\Delta\Delta Ct$ method. All reactions were performed in triplicates, and each experiment was repeated with at least three independent preparations of RNA.

ChIP Assays—ChIP assays were performed using a commercially available kit (Millipore, Billerica, MA) (10, 16). The "ChIPed" DNA was quantified using qPCR, with primers specific for the *DAPK1* promoter (40). DNA from total soluble chromatin was used as a template for PCR for determining input levels. Five micrograms of antibody was used for ChIPs with either an NR-IgG or specific IgG. No IgG and NR-IgG served as negative controls and defined the baselines.

Western Blotting Analysis—Whole cell extracts were fractionated by loading equal amounts of total protein on SDS-PAGE and transferred to polyvinylidene difluoride membranes. Western blots were probed with the indicated primary antibodies (1:1000 dilution) overnight at 4 °C. They were washed and probed with Alexa Fluor-tagged secondary antibodies (1:2000 dilution) for 1 h at room temperature. Blots were imaged using the LI-COR Odyssey infrared imaging system (10, 16). Mean intensities of the appropriate bands from three separate blots were quantified using the software provided by the manufacturer and ImageJ software (National Institutes of Health). Background intensities were subtracted and normalized to actin levels. Only representative images are shown. *Vertical lines* in the blot images indicate

TABLE 3
Gene-specific shRNA used in knockdown studies

shRNA	Mature antisense (5′ → 3′)
hDAPK1	ATTACATGCTTCTCAGGACAG
hCEBPB	TGTGTACAGATGAATGATAAA
hATF6	GGCAGCAACCAATTATCAGTTT

that the figure was recomposed from relevant lanes of the same blots after removing unrelated parts.

RNAi and Overexpression Analysis of DAPK1, C/EBP-β, and ATF6—Lentiviral vectors carrying short hairpin RNAs (shRNAs) specific for human *DAPK1*, *CEBPB*, and *ATF6* were from Open Biosystems, Inc. (Table 3). Virus stocks were prepared as recommended by the supplier and used as described in our earlier studies (10). Knockdown of the target gene products was assessed by Western blotting analyses. For overexpression, we transfected the indicated cells with expression vectors coding for either full-length human DAPK1, C/EBP-β, or ATF6 (10, 16) using Amaxa Nucleofector technology. To avoid potential overexpression artifacts, DNA transfection studies were performed with transgene expression levels corresponding to endogenous levels.

Immunofluorescence Microscopy—These analyses were conducted as described earlier (15, 16). Anti-LC3 (1:1000), anti-DAPK1 (1:500), anti-ATF6 (1:500), or anti-C/EBP-β (1:1000) was used as primary antibody, and Alexa Fluor- or FITC-conjugated anti-rabbit IgG (1:50) or anti-mouse IgG (1:50) was used as secondary antibody. Images were captured using a QICAM digital camera and were processed using Q-Capture Pro version 5.1 (Q-imaging). Mean intensities of fluorescent signals were quantified using ImageJ (National Institutes of Health).

Cell Viability Assay—Cells were plated in 24-well plates at 1×10^5 cells/well and treated either with IFN-γ or flavopiridol or chlorambucil for specific time points. Cell viability was measured by adding trypan blue and counting with a Cellometer Auto T4 counter (Nexcelom Bioscience, Lawrence, MA).

Statistical Analysis—Data were subjected to Student's *t* test, and $p < 0.05$ was considered significant.

Author Contributions—P. Gade, A. C. D., and P. Gangwal performed experiments. P. Gade, A. S. K., and D. V. K. designed the experiments. A. S. K. and D. D. R. collected the patient samples. P. Gade analyzed the data, and P. Gade and D. V. K. wrote the manuscript. S. K. K. and H. S. B. contributed toward reagents. H. S. B. discussed the results and the interpretations.

Acknowledgment—We thank Shreeram Nallar for proofreading the manuscript.

References

1. Harrison, B., Kraus, M., Burch, L., Stevens, C., Craig, A., Gordon-Weeks, P., and Hupp, T. R. (2008) DAPK-1 binding to a linear peptide motif in MAP1B stimulates autophagy and membrane blebbing. *J. Biol. Chem.* **283,** 9999–10014
2. Inbal, B., Bialik, S., Sabanay, I., Shani, G., and Kimchi, A. (2002) DAP kinase and DRP-1 mediate membrane blebbing and the formation of autophagic vesicles during programmed cell death. *J. Cell Biol.* **157,** 455–468
3. Gozuacik, D., Bialik, S., Raveh, T., Mitou, G., Shohat, G., Sabanay, H., Mizushima, N., Yoshimori, T., and Kimchi, A. (2008) DAP-kinase is a mediator of endoplasmic reticulum stress-induced caspase activation and autophagic cell death. *Cell Death Differ.* **15,** 1875–1886
4. Kissil, J. L., Feinstein, E., Cohen, O., Jones, P. A., Tsai, Y. C., Knowles, M. A., Eydmann, M. E., and Kimchi, A. (1997) DAP-kinase loss of expression in various carcinoma and B-cell lymphoma cell lines: possible implications for role as tumor suppressor gene. *Oncogene* **15,** 403–407
5. Galton, D. A. (1966) The pathogenesis of chronic lymphocytic leukemia. *Can. Med. Assoc. J.* **94,** 1005–1010
6. Reyes, E., Prieto, A., Carrión, F., García-Suarez, J., Esquivel, F., Guillén, C., and Alvarez-Mon, M. (1998) Altered pattern of cytokine production by peripheral blood $CD2^+$ cells from B chronic lymphocytic leukemia patients. *Am. J. Hematol.* **57,** 93–100
7. Zaki, M., Douglas, R., Patten, N., Bachinsky, M., Lamb, R., Nowell, P., and Moore, J. (2000) Disruption of the IFN-γ cytokine network in chronic lymphocytic leukemia contributes to resistance of leukemic B cells to apoptosis. *Leuk. Res.* **24,** 611–621
8. Thyrell, L., Hjortsberg, L., Arulampalam, V., Panaretakis, T., Uhles, S., Dagnell, M., Zhivotovsky, B., Leibiger, I., Grandér, D., and Pokrovskaja, K. (2004) Interferon α-induced apoptosis in tumor cells is mediated through the phosphoinositide 3-kinase/mammalian target of rapamycin signaling pathway. *J. Biol. Chem.* **279,** 24152–24162
9. Schmeisser, H., Fey, S. B., Horowitz, J., Fischer, E. R., Balinsky, C. A., Miyake, K., Bekisz, J., Snow, A. L., and Zoon, K. C. (2013) Type I interferons induce autophagy in certain human cancer cell lines. *Autophagy* **9,** 683–696
10. Gade, P., Roy, S. K., Li, H., Nallar, S. C., and Kalvakolanu, D. V. (2008) Critical role for transcription factor C/EBP-β in regulating the expression of death-associated protein kinase 1. *Mol. Cell Biol.* **28,** 2528–2548
11. Roy, S. K., Wachira, S. J., Weihua, X., Hu, J., and Kalvakolanu, D. V. (2000) CCAAT/enhancer-binding protein-β regulates interferon-induced transcription through a novel element. *J. Biol. Chem.* **275,** 12626–12632
12. Gonzalez-Gomez, P., Bello, M. J., Alonso, M. E., Lomas, J., Arjona, D., Amiñoso, C., De Campos, J. M., Isla, A., Gutierrez, M., and Rey, J. A. (2003) Frequent death-associated protein-kinase promoter hypermethylation in brain metastases of solid tumors. *Oncol. Rep.* **10,** 1031–1033
13. Gao, Y., Guan, M., Su, B., Liu, W., Xu, M., and Lu, Y. (2004) Hypermethylation of the RASSF1A gene in gliomas. *Clin. Chim. Acta* **349,** 173–179
14. Simpson, D. J., Clayton, R. N., and Farrell, W. E. (2002) Preferential loss of death associated protein kinase expression in invasive pituitary tumours is associated with either CpG island methylation or homozygous deletion. *Oncogene* **21,** 1217–1224
15. Gade, P., Ramachandran, G., Maachani, U. B., Rizzo, M. A., Okada, T., Prywes, R., Cross, A. S., Mori, K., and Kalvakolanu, D. V. (2012) An IFN-γ-stimulated ATF6-C/EBP-β-signaling pathway critical for the expression of death associated protein kinase 1 and induction of autophagy. *Proc. Natl. Acad. Sci. U.S.A.* **109,** 10316–10321
16. Gade, P., Manjegowda, S. B., Nallar, S. C., Maachani, U. B., Cross, A. S., and Kalvakolanu, D. V. (2014) Regulation of the death-associated protein kinase 1 expression and autophagy via ATF6 requires apoptosis signal-regulating kinase 1. *Mol. Cell Biol.* **34,** 4033–4048
17. Gozuacik, D., and Kimchi, A. (2007) Autophagy and cell death. *Curr. Top. Dev. Biol.* **78,** 217–245
18. Kubisch, J., Turei, D., Földvári-Nagy, L., Dunai, Z. A., Zsákai, L., Varga, M., Vellai, T., Csermely, P., and Korcsmáros, T. (2013) Complex regulation of autophagy in cancer: integrated approaches to discover the networks that hold a double-edged sword. *Semin. Cancer Biol.* **23,** 252–261
19. Narayan, G., Arias-Pulido, H., Koul, S., Vargas, H., Zhang, F. F., Villella, J., Schneider, A., Terry, M. B., Mansukhani, M., and Murty, V. V. (2003) Frequent promoter methylation of CDH1, *DAPK*, *RARB*, and *HIC1* genes in carcinoma of cervix uteri: its relationship to clinical outcome. *Mol. Cancer* **2,** 24–36
20. Raval, A., Tanner, S. M., Byrd, J. C., Angerman, E. B., Perko, J. D., Chen, S. S., Hackanson, B., Grever, M. R., Lucas, D. M., Matkovic, J. J., Lin, T. S., Kipps, T. J., Murray, F., Weisenburger, D., Sanger, W., *et al.* (2007) Down-

regulation of death-associated protein kinase 1 (DAPK1) in chronic lymphocytic leukemia. *Cell* **129,** 879–890
21. Moscat, J., Diaz-Meco, M. T., and Wooten, M. W. (2007) Signal integration and diversification through the p62 scaffold protein. *Trends Biochem. Sci.* **32,** 95–100
22. Zalckvar, E., Berissi, H., Mizrachy, L., Idelchuk, Y., Koren, I., Eisenstein, M., Sabanay, H., Pinkas-Kramarski, R., and Kimchi, A. (2009) DAP-kinase-mediated phosphorylation on the BH3 domain of beclin 1 promotes dissociation of beclin 1 from Bcl-XL and induction of autophagy. *EMBO Rep.* **10,** 285–292
23. Shanmugam, R., Gade, P., Wilson-Weekes, A., Sayar, H., Suvannasankha, A., Goswami, C., Li, L., Gupta, S., Cardoso, A. A., Al Baghdadi, T., Sargent, K. J., Cripe, L. D., Kalvakolanu, D. V., and Boswell, H. S. (2012) A noncanonical Flt3ITD/NF-κB signaling pathway represses DAPK1 in acute myeloid leukemia. *Clin. Cancer Res.* **18,** 360–369
24. Tamura, T., Nagamura-Inoue, T., Shmeltzer, Z., Kuwata, T., and Ozato, K. (2000) ICSBP directs bipotential myeloid progenitor cells to differentiate into mature macrophages. *Immunity* **13,** 155–165
25. Kamijo, R., Harada, H., Matsuyama, T., Bosland, M., Gerecitano, J., Shapiro, D., Le, J., Koh, S. I., Kimura, T., and Green, S. J. (1994) Requirement for transcription factor IRF-1 in NO synthase induction in macrophages. *Science* **263,** 1612–1615
26. Sedlacek, H., Czech, J., Naik, R., Kaur, G., Worland, P., Losiewicz, M., Parker, B., Carlson, B., Smith, A., Senderowicz, A., and Sausville, E. (1996) Flavopiridol (L86 8275; NSC 649890), a new kinase inhibitor for tumor therapy. *Int. J. Oncol.* **9,** 1143–1168
27. Begleiter, A., Mowat, M., Israels, L. G., and Johnston, J. B. (1996) Chlorambucil in chronic lymphocytic leukemia: mechanism of action. *Leuk. Lymphoma* **23,** 187–201
28. Mahoney, E., Lucas, D. M., Gupta, S. V., Wagner, A. J., Herman, S. E., Smith, L. L., Yeh, Y. Y., Andritsos, L., Jones, J. A., Flynn, J. M., Blum, K. A., Zhang, X., Lehman, A., Kong, H., Gurcan, M., *et al.* (2012) ER stress and autophagy: new discoveries in the mechanism of action and drug resistance of the cyclin-dependent kinase inhibitor flavopiridol. *Blood* **120,** 1262–1273
29. Panasci, L., Paiement, J. P., Christodoulopoulos, G., Belenkov, A., Malapetsa, A., and Aloyz, R. (2001) Chlorambucil drug resistance in chronic lymphocytic leukemia: the emerging role of DNA repair. *Clin. Cancer Res.* **7,** 454–461
30. Klionsky, D. J. (2007) Autophagy: from phenomenology to molecular understanding in less than a decade. *Nat. Rev. Mol. Cell Biol.* **8,** 931–937
31. Hoare, M., Young, A. R., and Narita, M. (2011) Autophagy in cancer: having your cake and eating it. *Semin. Cancer Biol.* **21,** 397–404
32. Young, A. R. J., Narita, M., Ferreira, M., Kirschner, K., Sadaie, M., Darot, J. F. J., Tavaré, S., Arakawa, S., Shimizu, S., Watt, F. M., and Narita, M. (2009) Autophagy mediates the mitotic senescence transition. *Genes Dev.* **23,** 798–803
33. Delmas, D., Solary, E., and Latruffe, N. (2011) Resveratrol, a phytochemical inducer of multiple cell death pathways: apoptosis, autophagy and mitotic catastrophe. *Curr. Med. Chem.* **18,** 1100–1121
34. Galluzzi, L., Bravo-San Pedro, J. M., and Kroemer, G. (2016) Autophagy mediates tumor suppression via cellular senescence. *Trends Cell Biol.* **26,** 1–3
35. Subramani, S., and Malhotra, V. (2013) Non-autophagic roles of autophagy-related proteins. *EMBO Rep.* **14,** 143–151
36. Zalckvar, E., Berissi, H., Eisenstein, M., and Kimchi, A. (2009) Phosphorylation of Beclin 1 by DAP-kinase promotes autophagy by weakening its interactions with Bcl-2 and Bcl-XL. *Autophagy* **5,** 720–722
37. Bialik, S., and Kimchi, A. (2014) The DAP-kinase interactome. *Apoptosis* **19,** 316–328
38. Eisenberg-Lerner, A., and Kimchi, A. (2012) PKD is a kinase of Vps34 that mediates ROS-induced autophagy downstream of DAPk. *Cell Death Differ.* **19,** 788–797
39. Zhao, J., Zhao, D., Poage, G. M., Mazumdar, A., Zhang, Y., Hill, J. L., Hartman, Z. C., Savage, M. I., Mills, G. B., and Brown, P. H. (2015) Death-associated protein kinase 1 promotes growth of p53-mutant cancers. *J. Clin. Invest.* **125,** 2707–2720
40. Gade, P., Singh, A. K., Roy, S. K., Reddy, S. P., and Kalvakolanu, D. V. (2009) Down-regulation of the transcriptional mediator subunit Med1 contributes to the loss of expression of metastasis-associated dapk1 in human cancers and cancer cells. *Int. J. Cancer* **125,** 1566–1574
41. Chiorazzi, N., Rai, K. R., and Ferrarini, M. (2005) Chronic lymphocytic leukemia. *N. Engl. J. Med.* **352,** 804–815
42. Moscat, J., and Diaz-Meco, M. T. (2009) p62 at the crossroads of autophagy, apoptosis, and cancer. *Cell* **137,** 1001–1004
43. Komatsu, M., Kageyama, S., and Ichimura, Y. (2012) p62/SQSTM1/A170: physiology and pathology. *Pharmacol. Res.* **66,** 457–462
44. Rutkowski, D. T., and Kaufman, R. J. (2004) A trip to the ER: coping with stress. *Trends Cell Biol.* **14,** 20–28
45. Haze, K., Yoshida, H., Yanagi, H., Yura, T., and Mori, K. (1999) Mammalian transcription factor ATF6 is synthesized as a transmembrane protein and activated by proteolysis in response to endoplasmic reticulum stress. *Mol. Biol. Cell* **10,** 3787–3799
46. Shen, J., Chen, X., Hendershot, L., and Prywes, R. (2002) ER stress regulation of ATF6 localization by dissociation of BiP/GRP78 binding and unmasking of Golgi localization signals. *Dev. Cell* **3,** 99–111
47. Baumeister, P., Luo, S., Skarnes, W. C., Sui, G., Seto, E., Shi, Y., and Lee, A. S. (2005) Endoplasmic reticulum stress induction of the Grp78/BiP promoter: activating mechanisms mediated by YY1 and its interactive chromatin modifiers. *Mol. Cell Biol.* **25,** 4529–4540
48. Harding, H. P., Calfon, M., Urano, F., Novoa, I., and Ron, D. (2002) Transcriptional and translational control in the mammalian unfolded protein response. *Annu. Rev. Cell Dev. Biol.* **18,** 575–599
49. Chen, K. G., and Sikic, B. I. (2012) Molecular pathways: regulation and therapeutic implications of multidrug resistance. *Clin. Cancer Res.* **18,** 1863–1869
50. Furuya, T., Kim, M., Lipinski, M., Li, J., Kim, D., Lu, T., Shen, Y., Rameh, L., Yankner, B., Tsai, L. H., and Yuan, J. (2010) Negative regulation of Vps34 by Cdk mediated phosphorylation. *Mol. Cell* **38,** 500–511
51. Galluzzi, L., Pietrocola, F., Bravo-San Pedro, J. M., Amaravadi, R. K., Baehrecke, E. H., Cecconi, F., Codogno, P., Debnath, J., Gewirtz, D. A., Karantza, V., Kimmelman, A., Kumar, S., Levine, B., Maiuri, M. C., Martin, S. J., *et al.* (2015) Autophagy in malignant transformation and cancer progression. *EMBO J.* **34,** 856–880
52. Buggins, A. G., Pepper, C., Patten, P. E., Hewamana, S., Gohil, S., Moorhead, J., Folarin, N., Yallop, D., Thomas, N. S., Mufti, G. J., Fegan, C., and Devereux, S. (2010) Interaction with vascular endothelium enhances survival in primary chronic lymphocytic leukemia cells via NF-κB activation and *de novo* gene transcription. *Cancer Res.* **70,** 7523–7533
53. Burger, J. A., Quiroga, M. P., Hartmann, E., Bürkle, A., Wierda, W. G., Keating, M. J., and Rosenwald, A. (2009) High-level expression of the T-cell chemokines CCL3 and CCL4 by chronic lymphocytic leukemia B cells in nurselike cell cocultures and after BCR stimulation. *Blood* **113,** 3050–3058
54. Lagneaux, L., Delforge, A., Bron, D., De Bruyn, C., and Stryckmans, P. (1998) Chronic lymphocytic leukemic B cells but not normal B cells are rescued from apoptosis by contact with normal bone marrow stromal cells. *Blood* **91,** 2387–2396
55. Os, A., Bürgler, S., Ribes, A. P., Funderud, A., Wang, D., Thompson, K. M., Tjønnfjord, G. E., Bogen, B., and Munthe, L. A. (2013) Chronic lymphocytic leukemia cells are activated and proliferate in response to specific T helper cells. *Cell Rep.* **4,** 566–577
56. Bürgler, S., Gimeno, A., Parente-Ribes, A., Wang, D., Os, A., Devereux, S., Jebsen, P., Bogen, B., Tjønnfjord, G. E., and Munthe, L. A. (2015) Chronic lymphocytic leukemia cells express CD38 in response to Th1 cell-derived IFN-gamma by a T-bet-dependent mechanism. *J. Immunol.* **194,** 827–835
57. Burgler, S. (2015) Role of CD38 expression in diagnosis and pathogenesis of chronic lymphocytic leukemia and its potential as therapeutic target. *Crit. Rev. Immunol.* **35,** 417–432
58. So, A. Y., de la Fuente, E., Walter, P., Shuman, M., and Bernales, S. (2009) The unfolded protein response during prostate cancer development. *Cancer Metastasis Rev.* **28,** 219–223

59. Wu, X., Xin, Z., Zhang, W., Zheng, S., Wu, J., Chen, K., Wang, H., Zhu, X., Li, Z., Duan, Z., Li, H., and Liu, Y. (2014) A missense polymorphism in ATF6 gene is associated with susceptibility to hepatocellular carcinoma probably by altering ATF6 level. *Int. J. Cancer* **135,** 61–68
60. Tomizawa, M., Watanabe, K., Saisho, H., Nakagawara, A., and Tagawa, M. (2003) Down-regulated expression of the CCAAT/enhancer binding protein α and β genes in human hepatocellular carcinoma: a possible prognostic marker. *Anticancer Res.* **23,** 351–354
61. Perillo, N. L., Naeim, F., Walford, R. L., and Effros, R. B. (1993) The *in vitro* senescence of human T lymphocytes: failure to divide is not associated with a loss of cytolytic activity or memory T cell phenotype. *Mech. Ageing Dev.* **67,** 173–185
62. Stacchini, A., Aragno, M., Vallario, A., Alfarano, A., Circosta, P., Gottardi, D., Faldella, A., Rege-Cambrin, G., Thunberg, U., Nilsson, K., and Caligaris-Cappio, F. (1999) MEC1 and MEC2: two new cell lines derived from B-chronic lymphocytic leukaemia in prolymphocytoid transformation. *Leuk. Res.* **23,** 127–136